Engineering and Technology Journal
Journal homepage: engtechjournal.org

Experimental Investigation of Combined Effect of Particle Size and Stability of Al_2O_3-H_2O Nanofluid on Heat Transfer Augmentation Through Horizontal Pipe

Abdulhassan A. Karamallah [a]*, Hayder H. Abed [b]

[a] Mechanical Engineering Department, University of Technology. Baghdad, Iraq.
2005@uotechnology.edu.iq

[b] Mechanical Engineering Department, University of Technology, Baghdad, Iraq.

*Corresponding author.

Submitted: 07/04/2019 Accepted: 30/07/2019 Published: 25/04/2020

K E Y W O R D S

Nanofluids, Convective heat transfer, particle size effect, stability effect, turbulent flow

A B S T R A C T

The stability of nanofluid plays a rule in heat transfer growth for different engineering systems. The stability and particle size of Al2O3-H2O nanofluid effects on heat transfer are studied experimentally. Two particle sizes (20 and 50 nm) with (0.1, 0.5 and 1%) concentrations were prepared and tested under constant heat flux (1404 W) with fully developed turbulent flow through a horizontal pipe. The results show an increase in Nusselt number by 20.7% and 17.6% with 1 vol.% concentration for 20 and 50 nm, respectively compared to distilled water. Examined nanofluid showed improvement in Nu number by (30.3 and 23.5) % at 1 vol.% concentration compared to water. Obtained results show minor decrease in the pressure drop and friction factor with nanofluid after stability treatment. Different correlations between Nu number and friction factor relating to studied parameters were observed.

How to cite this article: A.A. Karamallah and H. H. Abed, "Experimental investigation of combined effect of particle size and stability of Al_2O_3-H_2O nanofluid on heat transfer augmentation through horizontal pipe," Engineering and Technology Journal, Vol. 38, Part A, No. 04, pp. 561-573, 2020.
DOI: https://doi.org/10.30684/etj.v38i4A.177

1. Introduction

Improve the thermal performance of the heat transfer fluids is important of which it has many benefits like the shrinking surface area of heat exchange, minimizing cost, and reducing drawn power. Generally, the heat transfer coefficient of the fluids (e.g. water, oil, ethylene glycol (EG) or ethylene glycol-water) is low because of the lower thermal conductivity compared to the solid materials that have high thermal conductivity by tens or hundred times [1]. By blending a little amount of small solid particles with a bulk of fluid, this can improve the fluid capacity of heat transfer performance.
This idea was introduced by Maxwell at year (1873) when he used micro-scale particle size with a bulk fluid and observed fast settling, channel clogging, parts erosion and high-pressure drop [2]. At

1995, the "Nanofluid" term appeared officially by Choi and Eastman [3] when they experimentally investigated the suspension of copper oxide-water (CuO-H_2O) and aluminum oxide-ethylene glycol/water nanofluid (Al_2O_3-EG/H_2O), their results showed a thermal augmentation by 20% in the heat transfer. Also, they demonstrated the term "effective thermal conductivity (knf/kbf)" which means the ratio between nanofluid to base fluid thermal conductivity. Nanofluid could be defined as a suspension consist of the bulk of fluid and nanoparticles sized less than 100×10-9 meter [4]. Bajestan et al. [5] studied experimentally and theoretically the heat transfer characteristics of titanium dioxide - water nanofluid with different concentrations, particle diameter and base fluid type (H_2O and EG: H_2O). Also, they solved fixed concentration from CetyleTrimethly Ammonium Bromide (CTAB) as a surfactant to maintain the suspension stability. The results of experiments showed that the best augmentation in heat transfer coefficient occurs with maximum particle loading and minimum particle size.

The heat transfer performance of magnesium oxide- distilled water nanofluid was investigated experimentally by Esfe. [6] using variant the nanoparticles size and volume loading under turbulent flow regime with constant wall temperature. The best performance appears at the smallest particle size and maximum volume fraction. The researcher reported that at a low Reynold number, the particle diameter approximately does not affect heat transfer augmentation. Kayhani et al. [7] examined the particle loading effect on the heat transfer coefficient of Al_2O_3-H_2O nanofluid flowing under a turbulent flow regime with constant heat flux. Their experiments indicated that the heat transfer coefficient augmented with increasing the volume particle loading. They also confirmed Pak and Cho claimed in that the ratio of the Nunf to Nuw stay unchanged with Reynold number increment.

The particle size effect of alumina–water nanofluid on the convective heat transfer characteristics investigated by Anoop et al. [8], under the laminar flow regime in the developed region with constant heat flux and two-particle size 45 and 150 nm. Their experiment showed that there was an enhancement in heat transfer performance of the nanofluid compared to the base fluid. The particles sized with 45 nm enhanced the heat transfer coefficient better than 145 nm particle size at the same Reynold value. Nguyen et al. [9] investigated the effect of Al_2O_3-H_2O nanofluid on the heat transfer coefficient under turbulent flow regime through the electronic cooling system to study the influence of particle surface area on the heat transfer. Their experiment showed an enhancement as the volume concentration increasing and particle size decreasing.

The particle size effect has been highlighted in many previous studies, but most of these studied dealt with the size effect of the particle on thermophysical properties, however, limited information about its effect on the heat transfer coefficient is available. The present work aims to study the effect of the volume concentration, particle size and stability treatment on the heat transfer augmentation by using the aluminum oxide (Al_2O_3) with distilled water (H_2O) nanofluid with two-particle size (20 and 50 nm) and three-volume concentration (0.1, 0.5 and 1%) for each particle size with and without altering the colloid pH under turbulent flow regime, Re (5000 - 10000) with 1000 interval.

Nomenclature

A: Surface area of the pipe (m^2).
Cp: Specific heat (J/kg.K)
D: Diameter (m)
f: Friction factor
H: Heat transfer coefficient ($W/m^2.K$)
I: Current (Amp)
K: Thermal conductivity (W/m.K)
L: Length (m)
L_e: Hydrodynamic entrance length (m)
ṁ: Mass flow rate (kg/s)
Ƥ: Circumference (m)
P: Pressure (Pa.s)
Q_H: Total heat power (W)
Q_{nf}: Heat gain by nanofluid (W)
q": Heat flux (W/m^2)
R: Pipe radius (m)

T: Temperature (℃)
T_m: Bulk temperature (℃)
T_s: Surface temperature (℃)
U: Velocity (m/s)
V: Voltage, volume (V)
ΔT_m: Mean temperature difference
{μ}: Dynamic viscosity (Pa.s)
{ν}: Kinematic viscosity (m^2/s)
{ρ}: Density (kg/s)
{φ}: Volume concentration (%)

2. Nanptofluid Preparation

Figures 1 and 2 shows the FESEM for 20 and 50 nm particle size of Al_2O_3, respectively. The nanofluid was prepared via two-step method [10] by adding the particles to the base fluid and blending the mixture by magnetic stirrer then using the ultrasonic probe type for 30 minutes to homogenize the colloid. Three volume concentration (0.1, 0.5 and 1%) for each particle size were prepared.

3. Stability Treatment

To treat the colloid stability, the pH-controlled to 5.5 and 5 for 20 and 50 nm particle size, respectively which represent the optimum value based on experimental tests. Figure 3 shows the zeta potential value for the suspension before and after stability treatment for each concentration. Altered pH has increased the zeta potential value for all concentrations and particle size as well as this value increased as concentration increases and particle size decreases. The best stability appeared at the highest volume concentration (1 vol.%) with 20 nm where the zeta potential is 41.85 mV and 40.05 mV for 50 nm.

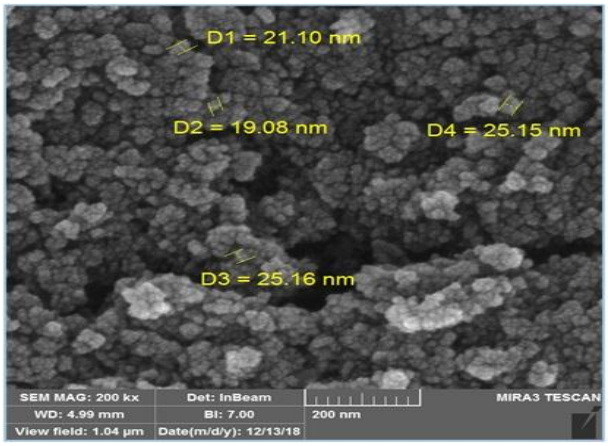

Figure 1: FESEM images for alumina powder with 20 nm particle size

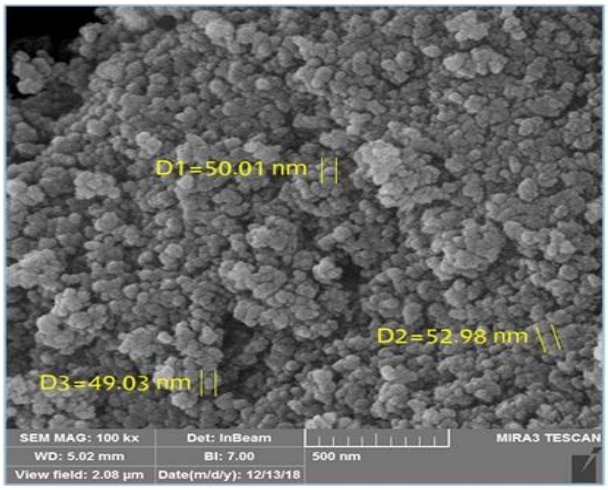

Figure 2: FESEM images for alumina powder with 50 nm particle size

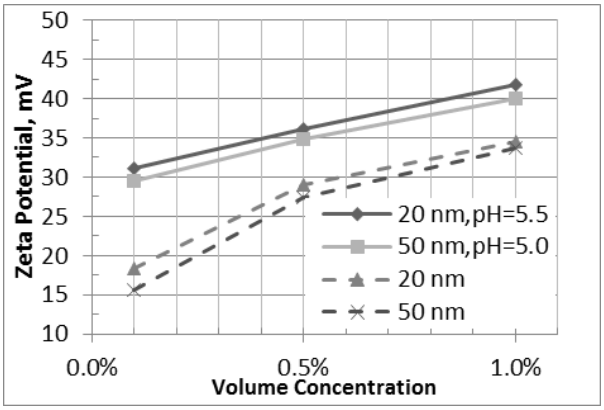

Figure 3: Volume concentration versus zeta potential of Al203-H2O nanofluid with and without optimum pH value

4. Experimental Test Rig

Heat transfer augmentation of the nanofluid was investigated experimentally through a test rig constructed for this purpose under constant heat flux (1404 W) at fully developed turbulent flow with Reynold number range (5000-10000).

The test rig consists of two cycles: nanofluid cycle and the cooling cycle. The main components of the nanofluid cycle are test section, heat exchanger, nanofluid reservoir and centrifugal pump. The cooling cycle included two water pumps and source tank, Figures 4 and 5.

The test section consists of copper pipe with 1.45 m, 10.7 mm and 1 mm as total length, inner diameter, and thickness, respectively, the test carried out through 1 m of the test section. An electrical heater type FeCrAl (Iron – Chromium - Aluminum) alloy wire with 0.8 mm diameter and 8.45 m length was used to generate a constant heat flux. Two types of insulation were used to reduce heat losses.

To measure the temperature along the test section, bolt and pressure spring thermocouples type K were used. Seven bolt thermocouples employed to measure the surface temperature at fully developed region with 12.5 cm apart between each other. The other two thermocouples fixed at the inlet and outlet of the test section to read the nanofluid temperature. Three flow meters were used, the first one is a flow sensor model YF-S201 working with Arduino technology with range (0 – 30 l/min) located after the nanofluid pump discharge. The other two flow meters are rotameters model YYXZ with (0 - 18 l/min) working range. One was located after the flow sensor to ensure the amount of the flow rate, the another was located on the bypass line in the cooling cycle. A differential pressure gauge Grundfos - Germany was used to measuring the pressure drop through the test section.

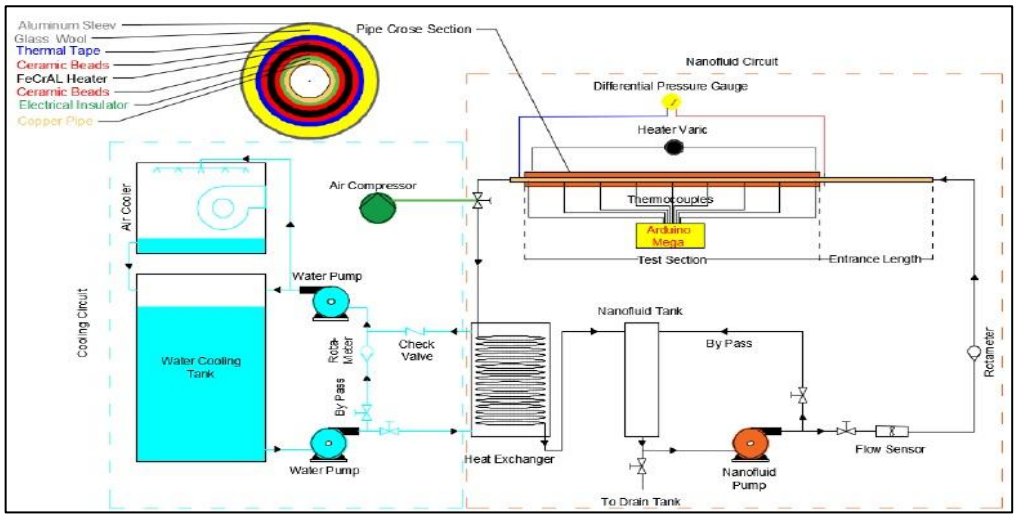

Figure 4: Schematic diagram of the test rig

Figure 5: Photo for the test rig

5. Data Processing

The heater is generating a constant heat on the outer surface of the pipe:

$$Q_{heater} = I \times V \quad (1)$$

Where I: current and V: voltage, the generated heat is transferred through the pipe wall by conduction according to Fourier's law [11]:

$$Q = \dot{q}A_{s,out} = 2\pi\Delta x k \frac{\left[T_{s,out}(x) - T_{s,in}(x)\right]}{\ln(r_{out}/r_{in})} \quad (2)$$

So, the heat flux on the outer surface of the pipe is given by:

$$\dot{q} = \frac{2k\left[T_{s,out}(x) - T_{s,in}(x)\right]}{D_o \ln(r_o/r_{in})} \quad (3)$$

The net heat flux that transferred to the nanofluid through the pipe wall is just taken under account into calculation. From Eq. (3) the heat flux and$T_{s,out}(x)$ are measured and $T_{s,in}(x)$will be calculated. The rate of heat transfer to the nanofluid is given by [11]:

$$Q_{nf} = \dot{q}A_{s,in} = \dot{m}_{nf}Cp_{nf}\left(T_{nf,out} - T_{nf,in}\right) \quad (4)$$

where, $A_{s,in} = \pi D_{in} L$ or Eq. (4) will be:

$$\dot{q} = \frac{\dot{m}_{nf}Cp_{nf}}{\pi D_{in} L}\left(T_{nf,out} - T_{nf,in}\right) \quad (5)$$

The differential mean fluid temperature can be written as:

$$dT_m = \frac{\dot{q}p}{\dot{m}Cp}dx \quad (6)$$

The local mean fluid temperature $T_m(x)$ can be determined by integration of Eq. (6) from $x = 0$ to x along the test section and assuming the$T_{m,in}$ at x=0 is equal to $T_{nf,in}$, or:

$$T_m(x) = T_{nf,in} + \frac{\dot{q}p}{\dot{m}Cp}x \quad (7)$$

Substitution Eq. (5) in Eq. (7), will get the value of local mean fluid temperature:

$$T_m(x) = T_{nf,in} + \frac{(T_{nf,out} - T_{nf,in})}{L} x \qquad (8)$$

According to Newton's law of cooling, the local heat transfer coefficient is:

$$h(x) = \frac{\dot{q}}{\left[T_{s,in}(x) - T_m(x)\right]} \qquad (9)$$

The fully developed region in the test section is divided into seven sections with a 12.5 cm distance between each section. The Nusselt number will be calculated locally at each section by the equation [12]:

$$Nu(x) = \frac{h(x) D_{in}}{k_{nf}} \qquad (10)$$

The efficiency of heat transfer from the heater (Q_h) to the nanofluid (Q_{nf}) across the test section layers ranged from (73% to 89%) and calculated by:

$$\eta_{th} = \frac{Q_{nf}}{Q_{heater}} \qquad (11)$$

6. Test Rig Validity

To confirm the experimental test rig validity in convective heat transfer calculations as well as to provide a reference for comparison, the first test was conducted on the distilled water only. The predicted Nusselt number calculated by Gnielinski equation [13] for turbulent fully developed flow compared to the present work versus Reynold number is shown in Figure 6. The experimental behavior was conformable to the predicted values with deviation from 11% to 23% due to the experimental actual conditions, Gnielinski equation is given by:

$$Nu = \frac{\left(\frac{f}{8}\right)(Re - 1000)Pr}{1 + 12.7\left(\frac{f}{8}\right)^{0.5}(Pr^{\frac{2}{3}} - 1)} \qquad (12)$$

where f is the friction factor for smooth surface and can be calculated from Petukhov equation;

$$f = (0.79 \ln Re - 1.64)^{-2} \qquad (13)$$

For, $3 \times 10^3 < Re < 5 \times 10^6$ and

$0.5 < Pr < 2000$

and Blasuius equation [11];

$$f = 0.316\, Re^{-0.25} \qquad (14)$$

The experimental friction factor is calculated from Darcy equation:

$$f = \frac{2\, \Delta P\, D}{L\, \rho\, V^2} \qquad (15)$$

Where; ΔP is the measured pressure drop through the test section. The comparison between calculated and experimental values versus Reynold number is given in Figure 7.

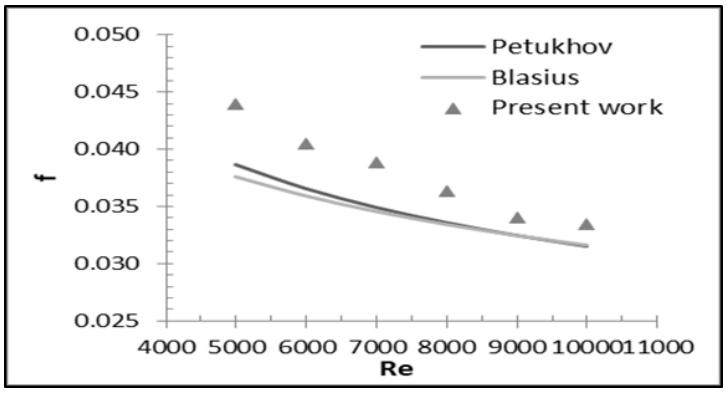

Figure 6: Experimental and theoretical Nusselt number for the distilled water

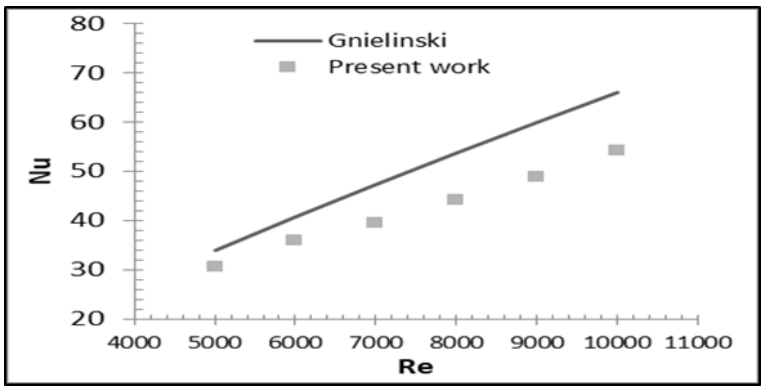

Figure 7: Experimental and theoretical friction factor for the distilled water

7. Thermophysical Properties

I. Density and specific heat measurement

The predicted nanofluid density and specific heat calculated based on the mixing theory:

$$\rho_{nf} = \varphi\rho_{np} + (1-\varphi)\rho_{bf} \quad (16)$$

$$Cp_{nf} = \frac{(1-\emptyset)(\rho Cp)_{bf} + (\emptyset\rho Cp)_p}{(1-\emptyset)(\rho)_{bf} + (\emptyset\rho)_p} \quad (17)$$

The nanofluid density was experimentally measured by using the pycnometer method. The specific heat of the nanofluid was measured based on the specific heat definition: 'the amount of heat required to raise the temperature of a unit mass of any substance through one degree'[14] by using the calorimeter vessel.

II. Viscosity measurement

The colloid viscosity plays a major role in estimating the application that uses it due to its directly related to the pumping power [15]. The predicted viscosity is calculated according to Batchelor model [16]:

$$\mu_{nf} = (1 + 2.5\varphi + 6.2\varphi^2)\mu_{bf} \quad (18)$$

The U tube viscometer was used to measure the experimental values.

III. Thermal conductivity measurement

The thermal conductivity is considered the core of the nanofluid field and the most important thermophysical property [17]. The thermal conductivity measurements of the used nanofluid were conducted by using the transient hot-wire techniques. Maxwell correlation was used to calculate the theoretical thermal conductivity [16]

$$k_{nf} = k_{bf}\left[\frac{\left(k_p + 2k_{bf}\right) + 2\emptyset(k_p - k_{bf})}{\left(k_p + 2k_{bf}\right) - \emptyset(k_p - k_{bf})}\right] \quad (19)$$

Thermophysical properties were measured experimentally at the mean temperature before and after stability treatment with two-particle size for three-volume concentrations and the results are listed in Table 1.

Table 1: Thermophysical properties of nanofluid before and after stability treatment

Particle Size, nm	Before stability treatment			After stability treatment		
	0.1%	**0.5%**	**1%**	**0.1%**	**0.5%**	**1%**
Density, kg/m^3						
20	994.0	1005.1	1013.1	993.4	1003.4	1010.9
50	994.9	1007.9	1014.2	994.2	1005.2	1012.1
Theoretical	995.0	1006.6	1021.2	995.0	1006.6	1021.2
Specific heat, J/kg.K						
20	4090.8	4051.4	3930.1	4110.2	4080.7	4027.1
50	4103.4	4073.4	4004.2	4127.4	4115.0	4064.3
Theoretical	4165.6	4112.9	4048.6	4165.6	4112.9	4048.6
Viscosity, kg/m.s × 10^{-3}						
20	0.664	0.678	0.751	0.660	0.675	0.745
50	0.661	0.671	0.735	0.662	0.670	0.730
Theoretical	0.655	0.661	0.670	0.655	0.661	0.670
Thermal conductivity, W/m.K						
20	0.637	0.652	0.678	0.642	0.661	0.695
50	0.635	0.648	0.670	0.641	0.657	0.687
Theoretical	0.633	0.643	0.656	0.633	0.643	0.656

8. Results and Discussion

I. Stable Nanofluid effect on Thermal Characteristics

Using nanofluid showed an augmentation in the local heat transfer coefficient compared with the distilled water under the same experimental conditions. The average heat transfer coefficient versus Reynold number was explained in Figures 8 and 9 for the nanofluid before and after stability treatment, respectively.

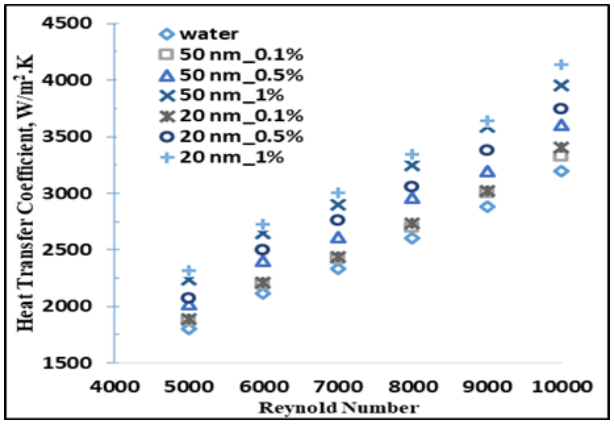

Figure 8: Average heat transfer coefficient for water and Al_2O_3-H_2O nanofluid before stability treatment

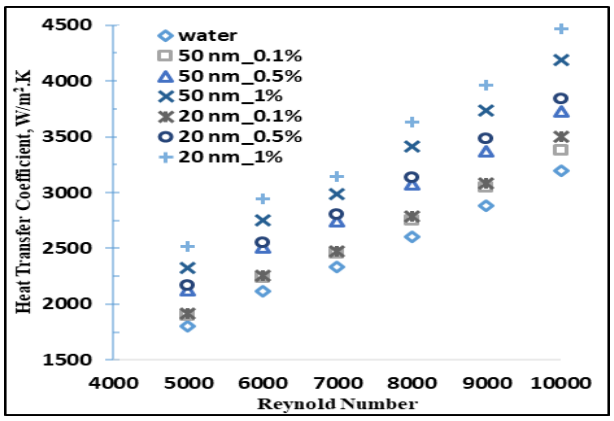

Figure 9: Average heat transfer coefficient for water and Al_2O_3-H_2O nanofluid after stability treatment

The results indicate an augmentation in the average heat transfer coefficient which increases as particle loading increase and particle size decrease at fixed Reynold number. The better performance in heat transferring related to the ability of nanofluid in absorbing the heat from the pipe wall due to the nanoparticle's thermal conductivity improvement. Therefore this leads to an increase in the heat gain by the nanofluid and decreasing the differences between the surface temperature and transportation medium. The best heat transfer enhancement was 29.6% where appeared at 1%, 20 nm and 10000 for particle loading, particle size, and Reynold number, respectively. The stable nanofluid gives better behavior than the unstable one where the enhancement reached 40%.

In Figures 10 and 11, the enhancement in the average heat transfer coefficient reflected the Nusselt number where the maximum augmented was 20.7% at 1%, 20 and 10000 for particle loading, particle size, and Reynold number, respectively. The enhancement in the Nusselt number for all nanofluid at three concentrations (0.1, 0.5 and 1%) were: 3.7%, 10.7% and 17.6%

for 50 nm and 5.6%, 14.4% and 20.7% for 20 nm before stability treated and there is no significant effect for the particle size on the heat transfer augmentation at the lowest concentration (0.1 vol.%) with the lower Reynold numbers. The enhancement became 5.3%, 15.4% and 23.5% for 50 nm and 8.1%, 16.7% and 30.3% for 20 nm after stability treated. The increment in the specific heat and thermal conductivity leads to increase the amount of heat gained by the nanofluid.

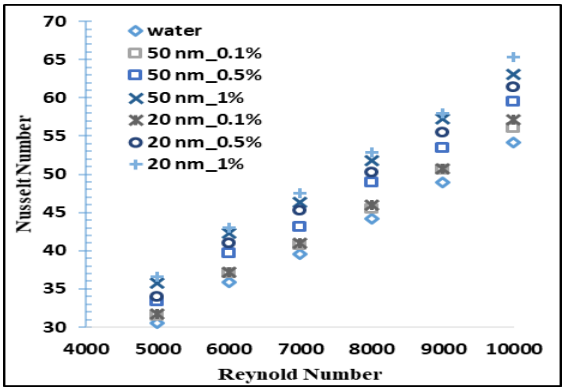

Figure 10: Average Nusselt number for water and Al_2O_3-H_2O nanofluid before stability treatment

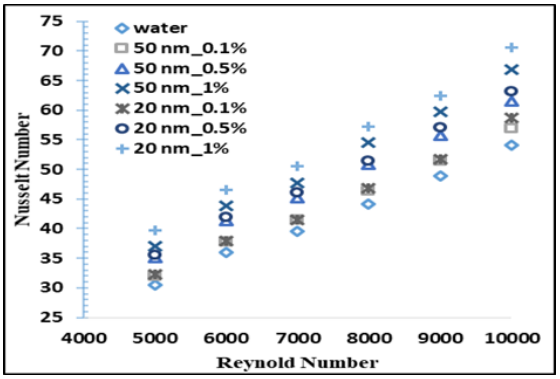

Figure 11: Average Nusselt number for water and Al2O3-H2O nanofluid after stability treatment

II. Stable Nanofluid Effect on Hydrodynamic Characteristic

The pressure drop in the test section was experimentally measured for the water and nanofluid at different Reynold numbers as shown in Figure 12. Adding nanoparticles to the base fluid increased the pressure drop compared to water. It was found an increment in the pressure drop as the concentration and Reynold number increasing with particle size decreasing due to the higher viscosity of the smallest particle size. The altered nanofluid showed lower pressure drop through the test section due to the enhancement in the thermophysical properties. In general, at lower Reynold number there are no significant differences in the pressure drop but will be more significant as the Reynold number and particle loading increase. The behavior of the friction factor versus Reynold number is illustrated in Figure 13. As the volume concentration increase and Reynold number decrease, the friction factor increases.

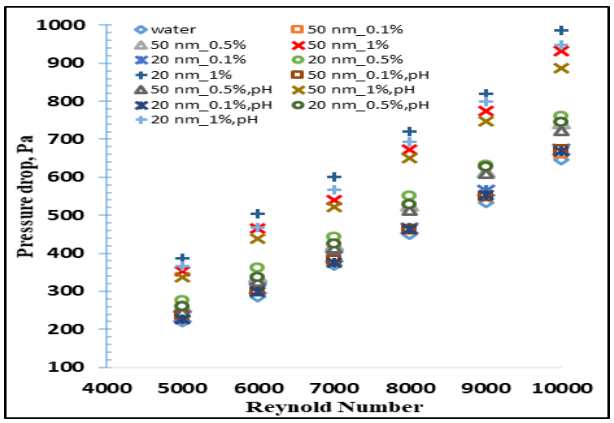

Figure 12: Pressure drop for Al_2O_3-H_2O nanofluid before and after stability treatment

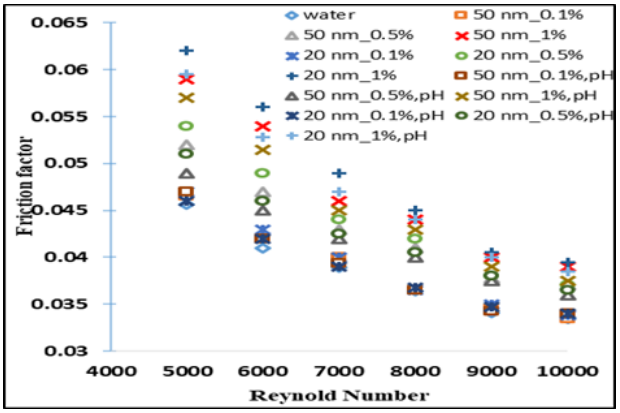

Figure 13: Friction factor for Al_2O_3-H_2O nanofluid before and after stability treatment

The maximum increment in the friction factor was 36.0% and 29.4% without stability treatment while became 30.5% and 25.0% with stability treatment for 50 nm and 20 nm particle size, respectively, which appeared at the same concentration 1 vol.% and Reynold number equal to 5000 compared to the distilled water. The density and viscosity enhanced due to stability treatment which leads to a pressure drop, this is , in turn, cause a decrease in the friction factor.

III. Nanofluid to Water Nusselt Number

The ratio of the nanofluid to the water Nusselt number (Nu_{nf}/Nu_{bf}) was introduced in Figure 14. The increment ratio is approximately constant versus Reynold number and this agreed with the claim of [7].

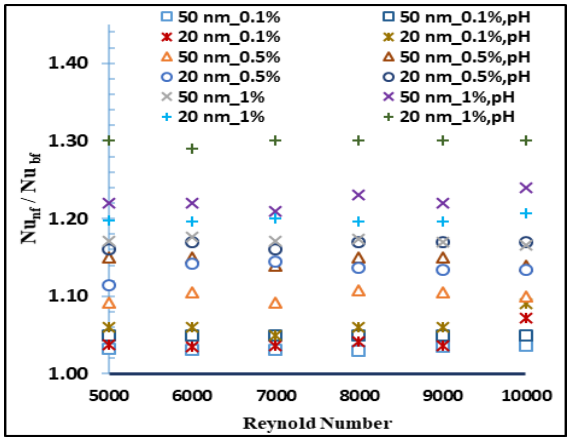

Figure 14: Nusselt number of nanofluid to base fluid ratio before and after stability treatment

Adding nanoparticles to the base fluid will increase the thermal conductivity and that will have enhanced the thermal performance for the nanofluid. But at the same time, nanoparticles increasing the suspension viscosity due to the increase in the thickness of the boundary layer which conflict and decreased the heat transfer coefficient. the results of the present work indicated an overcome of the thermal conductivity enhancement on the viscosity increment.
The present results were compared with the published work given in [7] for the heat transfer performance (Nusselt number) as shown in Figure 15. The maximum and minimum deviation were found at 23.6% and 15.5%. There is a small deviation between the results of the present work with the work of [7] because they achieved to 22% enhancement at Re = 13600 while we get on 20.7% at Re = 10000.

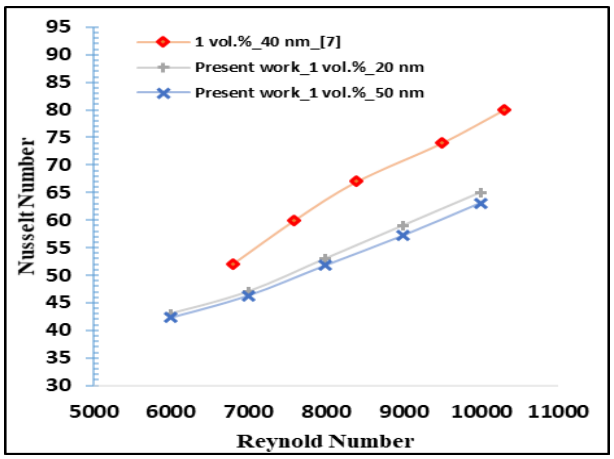

Figure 15: Comparison of the present experimental work with work of [7] for Nusselt number

9. Correlations

Correlation coefficients were developed for the Nusselt number and friction factor related to volume concentration (φ), particle size (dnp), Reynold number (Re) and Prandtl number (Pr) using the Statistical Package for the Social Sciences (SPSS 22) software.
1) The correlation to predict the Nusselt number is given by:

$$Nu = \beta_1(\varphi) + \beta_2(dnp)\beta_3 + \beta_4(\ln(Re))\beta_5 + \beta_6(Pr)$$

for,

$$0 \leq \emptyset \leq 0.01, \quad 20 \leq d_{np} \leq 50,$$

$$5000 \leq Re \leq 10000, 4.19 \leq Pr \leq 4.32$$

The values of constants are;
β_1= 844.485197, β_2=-0.000002, β_3= 3.298999, β_4=0.000260, β_5=5.654108, β_6=-4.072301
2) The correlation to predict the friction factor is given by:

$$f = \beta_1(\varphi)\beta_2 + \beta_3(dnp)\beta_4 + \beta_5(\ln(Re))\beta_6 + \beta_7(Pr)$$

for, $0 \leq \emptyset \leq 0.01, 20 \leq d_{np} \leq 50,$

$$5000 \leq Re \leq 10000, 4.19 \leq Pr \leq 4.32$$

The values of constants are;
β_1=0.920429221, β_2=1.015410810,
β_3=-0.000000001, β_4=3.451087874, β_5=88.135673, β_6=-3.314903, β_7=-0.00576
Figure 16. a, b shows the comparison between the correlated and predicted values for Nusselt number and friction factor with maximum error 8.1% and 8%, respectively.

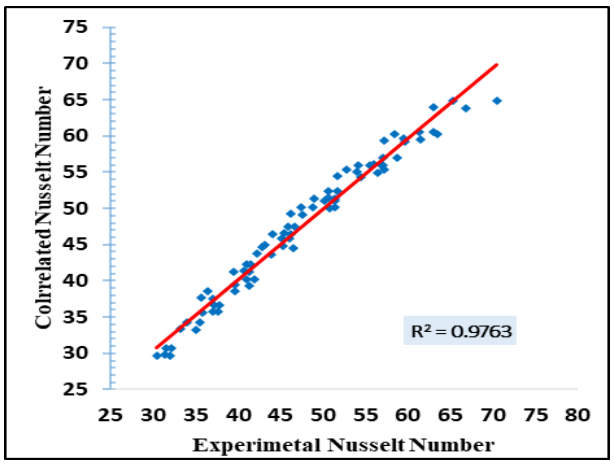

Figure 16-a: Comparison of experimental and correlated Nusselt number

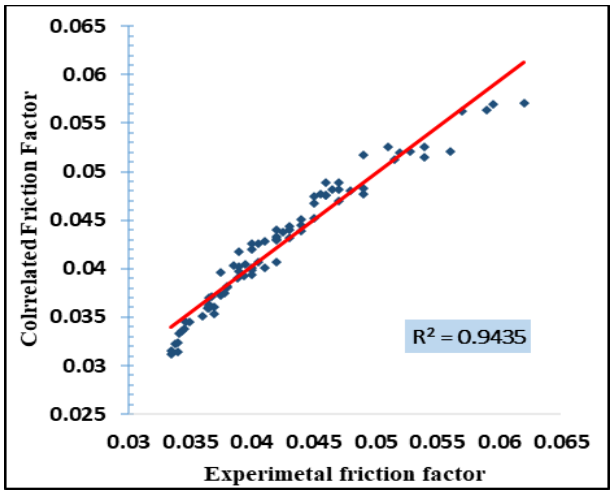

Figure 16-b: Comparison of experimental and correlated friction factor

10. Conclusions

1.Adding nanoparticles to the distilled water enhanced the heat transfer characteristic compared with distilled water through all Reynold number range.
2. Nanofluid stability caused more progress in the heat transfer performance where the Nusselt number augmentation became 46.3% and 33.5% for 20 nm and 50 nm particle size, respectively at 1 vol.% compared with the nanofluid without stability treatment.
3.As the particle size decreased and volume concentration increased the convective heat transfers increases.
4. The friction factor for the Al_20_3-H_2O nanofluid was higher than the suspension with stability treatment due to the viscosity and density decrement.

References

[1] P. Keblinski, S. R. Phillpot, S. U. S. Choi, and J. A. Eastman, "Mechanisms of heat flow in suspensions of nano-sized particles (nanofluids)," Int. J. Heat Mass Transf., vol. 45, pp. 855–863, 2002.

[2] J. C. Maxwell and J. J. Thompson, "A treatise on electricity and magnetism," vol. 2. Clarendon, 1904.

[3] J. A. Eastman, S. U. S. Choi, S. Li, W. Yu, and L. J. Thompson, "Anomalously increased effective thermal conductivities of ethylene glycol- based nanofluids containing copper nanoparticles," Appl. Phys. Lett., vol. 718, No. 6, pp. 4–7, 2012.

[4] S. Hasan, "A review on nanoparticles: their synthesis and types," Res. J. Recent. Sci., vol. 4, pp. 7–10, 2015.

[5] E. Ebrahimnia-Bajestan, M. Charjouei Moghadam, H. Niazmand, W. Daungthongsuk, and S. Wongwises, "Experimental and numerical investigation of nanofluids heat transfer characteristics for application in solar heat exchangers," Int. J. Heat Mass Transf., vol. 92, pp. 1041–1052, 2016.

[6] M. Hemmat Esfe and S. Saedodin, "Turbulent forced convection heat transfer and thermophysical properties of MgO-water nanofluid with consideration of different nanoparticles diameter, an empirical study," J. Therm. Anal. Calorim., vol. 119, pp. 1205–1213, 2015.

[7] M. H. Kayhani, M. Nazari, H. Soltanzadeh, M. M. Heyhat, and F. Kowsary, "Experimental analysis of turbulent convective heat transfer and pressure drop of Al_2O_3/water nanofluid in horizontal tube," Micro Nano Lett., vol. 7, p. 223, 2012.

[8] K. B. Anoop, T. Sundararajan, and S. K. Das, "Effect of particle size on the convective heat transfer in nanofluid in the developing region," Int. J. Heat Mass Transf., vol. 52, pp. 2189–2195, 2009.

[9] C. T. Nguyen, G. Roy, C. Gauthier, and N. Galanis, "Heat transfer enhancement using Al_2O_3-water nanofluid for an electronic liquid cooling system," Appl. Therm. Eng., vol. 27, no. 8–9, pp. 1501–1506, 2007.

[10] D. Dey, P. Kumar and S. Samantaray, "A review of nanofluid preparation, stability, and thermo-physical properties," Heat Transfer-Asian Res., vol. 46, pp. 1413–1442, 2017.

[11] Yunus A. Cengel, "Heat transfer a practical approach," Mcgraw-Hill, 2nd edition, 2002.

[12] Y. Kwon, K. Lee, M. Park, K. Koo, J. Lee, Y. Doh, S. Lee, D. Kim and Y. Jung, "Temperature dependence of convective heat transfer with nanofluids in the turbulent flow region," J. Nanosci. Nanotechnol., vol. 13, pp. 7902–7905, 2013.

[13] V. Gnielinski, "New equations for heat and mass transfer in turbulent pipe and channel flow," Int. Chem. Eng., vol. 16, no. 2, pp. 359–368, 1976.

[14] R. S. Khurmi and J. K. Gupta, "A textbook of thermal engineering," S. CHAND& COMPANY LTD., 34th ed, New Delhi, 2012.

[15] S. Murshed and P. Estellé, "A state of the art review on viscosity of nanofluids," Renew. Sustain. Energy Rev., vol. 76, pp. 1134–1152, 2017.

[16] X. Wang and A. S. Mujumdar, "A review on nanofluids - Part I: Theoretical and numerical investigations," Bra. J. Chem. Eng., vol. 25, pp. 613–630, 2008.

[17] H. A. Mohammeda, G. Bhaskarana, N. H. Shuaiba, and R. Saidur, "Heat transfer and fluid flow characteristics in microchannels heat exchanger using nanofluids: a review," Renew. Sustain. Energy Rev., vol. 15, pp. 1502–1512, 2011.